

# Autocrine-controlled formation and function of tissue-like aggregates by primary hepatocytes in micropatterned hydrogel arrays

Courtney M. Williams, PhD<sup>1†</sup>, Geeta Mehta, PhD<sup>1†</sup>, Shelly R. Peyton, PhD<sup>1</sup>, Adam S. Zeiger<sup>2</sup>, Krystyn J. Van Vliet, PhD<sup>1,2</sup>, Linda G. Griffith, PhD<sup>1,3,4,5</sup>

<sup>1</sup>Department of Biological Engineering, <sup>2</sup>Department of Materials Science and Engineering, <sup>3</sup>Biotechnology Process Engineering Center, <sup>4</sup>Department of Mechanical Engineering, Massachusetts Institute of Technology, 77 Massachusetts Avenue, 16-429, Cambridge, MA, 02139, USA.

<sup>5</sup>Corresponding author

† These authors contributed equally to this work.

Email: griff@mit.edu (LGG)

Phone: +1 617 253 0013 (LGG)

Fax: +1 617 253 2400 (LGG)

Courtney M. Williams, PhD  
Department of Biological Engineering, Massachusetts Institute of Technology,  
77 Massachusetts Avenue, 16-451, Cambridge, MA, 02139, USA.  
Email: courtney.m.williams@aya.yale.edu  
Phone: +1 617 253 7594  
Fax: +1 617 253 2400

Geeta Mehta, PhD  
Department of Biological Engineering, Massachusetts Institute of Technology,  
77 Massachusetts Avenue, 16-451, Cambridge, MA, 02139, USA.  
Email: mehtagee@umich.edu  
Phone: +1 517 303 1283  
Fax: +1 617 253 2400

Shelly R. Peyton, PhD  
Department of Biological Engineering, Massachusetts Institute of Technology,  
77 Massachusetts Avenue, 56-378, Cambridge, MA, 02139, USA.  
Email: speyton@mit.edu  
Phone: +1 617 258 0208  
Fax: +1 617 258 0204

Adam S. Zeiger  
Department of Materials Science & Engineering,  
Massachusetts Institute of Technology,  
77 Massachusetts Avenue, 8-235, Cambridge, MA, 02139, USA.  
Email: asz@mit.edu  
Phone: +1 617 253 0515  
Fax: +1 617 253 8745

Krystyn J. Van Vliet, PhD,  
Thomas Lord Associate Professor  
Department of Materials Science & Engineering  
Department of Biological Engineering  
Massachusetts Institute of Technology,  
77 Massachusetts Avenue, 8-237, Cambridge, MA, 02139, USA.  
Email: krystyn@mit.edu  
Phone: +1 617 253 3315  
Fax: +1 617 253 8745

Linda G. Griffith, PhD  
Department of Biological Engineering  
Department of Mechanical Engineering  
Biotechnology Process Engineering Center,  
Massachusetts Institute of Technology,  
77 Massachusetts Avenue, 16-429, Cambridge, MA, 02139, USA.  
Email: griff@mit.edu  
Phone: +1 617 253 0013  
Fax: +1 617 253 2400

**Abstract:**

The liver carries out a variety of essential functions regulated, in part by autocrine signaling, including hepatocyte-produced growth factors and extracellular matrix (ECM). The local concentrations of autocrine factors are governed by a balance between receptor-mediated binding at the cell surface and diffusion into the local matrix, and are thus expected to be influenced by the dimensionality of the cell culture environment. To investigate the role of growth factor and ECM-modulated autocrine signaling in maintaining appropriate primary hepatocyte survival, metabolic functions, and polarity, we created three-dimensional (3D) cultures of defined geometry using micropatterned semi-synthetic PEG-Fibrinogen hydrogels to provide a mechanically compliant, non-adhesive material platform that could be modified by cell-secreted factors. We found that in the absence of exogenous peptide growth factors or extracellular matrix, hepatocytes retain the epidermal growth factor receptor (EGFR) ligands EGF and TGF- $\alpha$ , and the c-MET ligand HGF, along with fibronectin. Further, hepatocytes cultured in this 3D microenvironment maintained high levels of liver-specific functions over the 10-day culture period. Function-blocking inhibitors of  $\alpha 5\beta 1$  or EGFR dramatically reduced cell viability and function, suggesting signaling by both these receptors is needed for *in vitro* survival and function of hepatocytes in the absence of other exogenous signals.

## Introduction:

Autocrine growth factor signaling by hepatocytes in the liver is a central mechanism for both physiological homeostasis and pathophysiological response of hepatocytes to stresses including inflammation and surgical resection. Epidermal growth factor receptor (EGFR) ligands, including Transforming Growth Factor- $\alpha$  (TGF- $\alpha$ ) and EGF, are produced by hepatocytes as well as non-parenchymal cells, and concentration gradients of these molecules influence a variety of cell behaviors in the intact liver (1). Extracellular matrix (ECM) molecules can also serve autocrine functions; for example, hepatocytes produce plasma fibronectin while also expressing its receptor  $\alpha 5 \beta 1$  integrin and the coreceptor syndecan-4 (2). Fibronectin (FN) fills the Space of Disse within the liver sinusoid, offering an adhesive matrix while allowing hepatocytes access to the circulating blood (3). Thus, *in vivo*, hepatocytes manipulate their microenvironment via production of autocrine factors essential to their survival and function, in dynamic response to external cues.

Exogenous EGF or TGF- $\alpha$  is typically added to serum-free culture media to enhance hepatocyte survival and function, especially in 2D culture formats (4-9), and EGF enhances spontaneous formation of 3D spheroidal aggregates of adult hepatocytes cultured on minimally adhesive 2D substrates (10-13). Hepatocytes in 3D spheroidal floating aggregates secrete ECM, and exhibit long term maintenance of liver functions (11, 12, 14-19) compared to cells cultured in 2D formats, where addition of DMSO or other cell types is required for functional maintenance (20). Unlike insulin and other hormones added to serum-free cell culture media, hepatocytes produce autocrine EGFR ligands *in vitro* (6, 21). The need for additional exogenous EGFR ligands in 2D culture, or in the formation of spheroids from cells seeded on 2D culture substrates, may arise

from a failure of autocrine ligands to be retained locally; i.e., ligands produced by cells in 2D can readily diffuse into the medium before recapture by cell surface receptors (22).

The contribution of autocrine ligands to enhanced maintenance of liver-specific functions in 3D spheroidal cultures of hepatocytes is unclear. Spheroidal cultures are often characterized by a layer of cells with flattened morphology at the outer rim (23, 24), a phenomenon that may arise from gradients in diffusible autocrine growth factors (which may accumulate in the interior portion of the spheroid but diffuse freely from the surface into culture medium); from mechanical stresses associated with contraction and compaction of cells against a free surface; or loss of appropriate ECM, such as FN, at the outer boundaries.

Here, we investigate the roles of autocrine growth factors and ECM in fostering viability, function, and polarization in adult rat hepatocytes using an experimental micromolded gel system that controls the geometry of 3D cell aggregation, presents a diffusion barrier to loss of autocrine factors, provides an initially inert (to cell adhesion) template that can be altered by ECM deposition to engage cells mechanically with the substrate, and provides a mechanically-compliant environment that approximates the compliance of liver. Although collagen gels are serviceable for hepatocyte culture (20, 25), and have been widely used to create micropatterned environments for other cell types (26-28), hepatocyte adhesion to collagen via collagen-binding integrins induces cell signaling and phenotypes that might mask the effects of autocrine factors or drive cells to undesirable phenotypes (25, 29, 30). To foster engagement of cell adhesion by cell-secreted FN, while dampening adhesive interactions during initial stages following cell seeding, we therefore focused on a semi-synthetic gel comprising polyethylene glycol (PEG) linked to denatured fibrinogen (PEG-Fibrinogen). Unlike endothelial cells and other  $\alpha v \beta 3$  integrin-expressing cells, hepatocytes do not bind directly to fibrinogen, but may interact with fibrinogen indirectly through fibronectin, which both binds to fibrin and is also recognized by

$\alpha 5\beta 1$  receptors on hepatocytes (17, 31). As fibrinogen is denatured during the process to form PEG-Fibrinogen gels, the tertiary structure which typically prevents fibrinogen-FN interaction is lost, while the secondary structure of fibrinogen peptides characteristic of the native protein is evident in the PEG-modified state (32) and hence presumably can bind fibronectin. PEG-Fibrinogen gels are relatively easy to micromold via UV-crosslinking processes, and can be fabricated with mechanical properties comparable to liver (33-35); hence, these gels provide an attractive experimental system for controlling hepatocyte aggregation and local retention of ECM produced by hepatocytes. Their permeability and degradation properties can also be tailored over a wide range through inclusion of additional PEG diacrylate with the PEG-Fibrinogen macromer in the polymerization process (36).

Exploiting these advantages of micropatterned PEG-Fibrinogen hydrogels, this study probes the nature and action of autocrine loops in regulating survival and function of primary hepatocytes. Using a combination of immunostaining and function-blocking inhibitors, we demonstrate that primary hepatocytes in micromolded PEG-Fibrinogen gels retain autocrine growth factors (EGF, HGF, TGF- $\alpha$ ) and cell-derived matrix (fibronectin). These factors are necessary and sufficient to maintain hepatocyte differentiation in culture, as determined by cell morphology and metabolic function. This culture system may prove useful for analysis of other aspects of hepatocellular biology or as a platform to study hepatocyte metabolism of pharmacological agents.

## Materials and Methods:

**Culture of primary hepatocytes in micromolded gels.** Primary cells were isolated from male Fisher rats weighing between 150 and 250 grams as previously described (20). Following isolation, primary hepatocytes were resuspended in serum-free hepatocyte growth medium (HGM; low glucose DMEM supplemented with 4mg/L insulin, 100 nM Dexamethasone, 0.03g/L proline, 0.1g/L L-ornithine, 0.305g/L niacinamide, 2g/L D-(+)-galactose, 2g/L D-(+)-glucose, 1mM L-glutamine, 50mg/L gentamicin, 54.4  $\mu\text{g/L}$   $\text{ZnCl}_2$ , 75  $\mu\text{g/L}$   $\text{ZnSO}_4 \cdot 7\text{H}_2\text{O}$ , 20 $\mu\text{g/L}$   $\text{CuSO}_4 \cdot 5\text{H}_2\text{O}$ , 25 $\mu\text{g/L}$   $\text{MnSO}_4$ ) without Epidermal Growth Factor (EGF) (37). Cells were plated onto micromolded gels at a density of 100,000 cells/cm<sup>2</sup> (720,000 cells/ml) in a 12-well tissue culture dish and spun at 100g for 3 minutes, this process was repeated twice. After seeding, gels were transferred to new wells with fresh HGM to remove excess cells. HGM was replaced after 24 hours and again after every fourth day of culture. Cells were incubated at 37°C, 5% CO<sub>2</sub> and 95% humidity for the time periods indicated, EGF was included in cultures at 10ng/ml as indicated. Medium was changed after 24 hours and again every four days for the duration of the cultures. For experiments with cyclic RGD peptide, 10 $\mu\text{M}$  of the peptide c(RGDfV) was included at the time of plating and maintained during culture (Peptides International). For experiments with EGFR inhibitor, 10 $\mu\text{M}$  of the monoclonal antibody mAb225 against EGFR was included at the time of plating and refreshed at each medium change (kind gift from H. Steve Wiley lab, PNNL). 24-well plates adsorbed with collagen I (BioCoat, BD Biosciences) with EGF containing HGM were used as controls in some experiments.

**Synthesis of PEG-Fibrinogen.** Poly(ethylene glycol) (PEG) was acrylated similar to previously published protocols (38, 39). Briefly, acryloyl chloride (Alfa Aesar, Ward Hill, MA) was reacted with PEG-diol (6 kDa or 10kDa, Sigma, St. Louis, MO) at 4x molar excess to available alcohol groups in benzene and under nitrogen pressure in the presence of triethylamine (Sigma) overnight at room temperature, protected from light. The resulting PEG-diacrylate (PEGDA)

product was purified by multiple rounds of diethyl ether precipitation, vacuum dried, lyophilized, and stored under nitrogen gas and at -20°C. Acrylation efficiency was determined by H-NMR and ranged from 85-95%.

Fibrinogen was PEGylated by reacting PEGDA (10kDa) with full-length fibrinogen in 4x molar excess to the number of cysteines on fibrinogen at room temperature in 8 M urea in PBS, pH 7.4, for 3h in the presence of tris(2-carboxyethyl)phosphine hydrochloride (Sigma) (39, 40). The PEGylated fibrinogen product was precipitated in acetone and dialyzed for 24 hr over 3 changes of PBS at 4C. The fibrinogen content of each batch of material was quantified with a BCA protein assay (Pierce Chemicals, Rockford, IL), and the PEG content was quantified by weighing the lyophilized product and subtracting out the contributions of PBS and fibrinogen (39). The fibrinogen content was  $7.2 \pm 0.2$  mg/ml and the PEG content was  $29 \pm 3.3$  mg/ml (both mean +/- s.e.).

**Micromolding of PEG-Fibrinogen gels.** Microwell patterns, a 5X7 array of 500µm diameter circles, were designed using AutoCAD (Autodesk, San Rafael, CA). A transparency mask was created from the CAD design and printed by a high-resolution printer (PageWorks, Cambridge, MA). The transparency mask was used in photolithography of SU-8 photoresist to create 200µm high patterns on the silicon wafer master. Micropatterned stamps were made by replica molding of polydimethylsiloxane (PDMS) (Sylgard 184) and curing the degassed elastomer mix (10:1, base: curing agent) over the silicon master overnight in a 60°C oven. Polymerized PDMS micropatterned stamps were peeled off the silicon master and used for patterning the PEG-Fibrinogen hydrogel. 100µl of a premixed solution containing PEG-Fibrinogen (3.6% wt/vol), 5% PEG-DA (MW=6 kDa) and 0.2% Irgacure 2959, was placed on the PDMS stamp, covered with a polycarbonate support scaffold (41) and cured under a handheld long-wave UV lamp, B-100YP

(UVP) for 4 minutes. Partially polymerized hydrogels were removed from PDMS stamps and cured with feature side up for one additional minute. PEG-DA (MW=6 kDa) micropatterned gels were made in the same manner with 0.2% Irgacure 2959. The resulting polymerized PEG-Fibrinogen or PEG-DA micropatterns were hydrated in PBS and UV sterilized before cell seeding. Measurements of PEG-Fibrinogen feature sizes done after hydration in PBS indicate microwells were  $522 \pm 27 \mu\text{m}$  in diameter and  $213 \pm 19 \mu\text{m}$  deep, measured by confocal imaging of microwells filled with  $20 \mu\text{m}$  diameter fluorescent beads (Figure 1).

### **Evaluation of mechanical properties of PEG-Fibrinogen hydrogels**

Polymer solutions that matched the composition of those used in cellular experiments, of approximately  $250 \mu\text{L}$  volume, were polymerized between 18mm coverslips. The bottom coverslip was functionalized with aminopropyltriethoxysilane to covalently link the hydrogel for ensuing testing. Several samples from four different PEG-Fibrinogen stocks were measured using atomic force microscopy-enabled nanoindentation. An atomic force microscope (AFM; MFP-3D, Asylum Research) was used for all mechanical characterization experiments conducted on hydrogels in 1X PBS at room temperature. Calibration of AFM cantilevers of spring constant  $k = 34.60 \text{ pN/nm}$  and nominal probe radius  $R = 25 \text{ nm}$  (MLCT, Veeco) was conducted as described previously (42, 43).

For each measurement of Young's elastic moduli, a grid of  $16 \times 16$  (256 total) indentations to maximum depths of  $25 \text{ nm}$  were acquired over a  $50 \mu\text{m}^2$  area on each hydrogel to account for material inhomogeneity. Acquired probe deflection-displacement responses were converted offline (Igor Pro, Wavemetrics), to force-depth responses. Young's elastic moduli  $E$  were calculated by applying a modified Hertzian model of spherical contact to the loading segment of the force-depth response, as detailed elsewhere (42, 43) with the scientific computing software MATLAB (2007a, TheMathWorks, Natick, MA). Computed elastic moduli  $E$  are reported as

average +/- standard error of measurement. The elastic modulus of the gels comprising 5% exogenous PEG diacrylate was  $17.5 \pm 0.3$  kPa (mean +/- s.e.m.), which is intermediate to that of estimates for normal and diseased liver as discussed in the text (33-35).

**Immunofluorescence microscopy:** Samples were fixed in 3.7% formaldehyde in phosphate buffered saline (PBS) for 25 minutes at room temperature, permeabilized with 0.1% Triton-X for 10 minutes at 4°C and washed with two changes of PBS for 15 minutes each. For accumulation of growth factors, samples were blocked for 1 hour with 10% normal goat serum (Invitrogen) and 1% Bovine Serum Albumin (Sigma). Samples were incubated with primary antibodies overnight at 4°C then washed with 3 changes of PBS for 20 minutes each. Samples were then incubated with secondary antibodies, AlexaFluor568 or AlexaFluor488 phalloidin, and DAPI or Hoechst nuclear stains for 1 hour at room temperature protected from light before being washed with 3 changes of PBS for 20 minutes each. Samples were then stored in PBS at 4°C, protected from light. Visualization was done using a Zeiss Observer A1 microscope equipped with a Photometrics Quant EM S12SC camera and BD CARV II spinning disc confocal (Biovision Technologies). Images were acquired using MetaMorph software. Confocal images shown in the Figures in this report are single confocal cross-sections taken within the centermost 25% of the tissue structure. Tissue structures were typically 180-200  $\mu\text{m}$  deep in the absence of inhibitors (and comparable for presence or absence of soluble EGF), 120-150  $\mu\text{m}$  deep (when intact) in the presence of cRGD integrin inhibitor, and 100-120  $\mu\text{m}$  deep in the presence of mAb225 EGFR inhibitor. Zeiss SteREO Discovery V12 stereoscope equipped with AxioCam and fluorescent lamp was used for observing accumulation of TGF- $\alpha$ , EGF and HGF in PEG-Fibrinogen microwells. Consistent exposure times were maintained to assess relative fluorescent staining between conditions. For EGF, TGF- $\alpha$  and HGF immunofluorescence, samples incubated with secondary antibody alone were imaged to ensure that the observed

fluorescence was not due to an artifact, such as non-specific secondary antibody binding or autofluorescence.

For visualization of functional bile canalicular networks, samples were washed three times with Hanks Balanced Salt Solution and then incubated for 10 minutes at 37°C with 2 $\mu$ M 5 (and 6)-carboxy-2',7'-dichlorofluorescein diacetate (CDFDA) (Invitrogen) and 16.2 $\mu$ M Hoechst stain. After incubation, confocal images were taken at day 3 and 6 (representative image from day 6 is depicted in Figure 5 E).

Primary antibodies include anti-rat fibronectin at 1:100 (Millipore), anti-rat CD26 at 1:100 (BD Pharmingen), anti-rat Transforming Growth Factor  $\alpha$  (TGF- $\alpha$ ) at 1:500 (Abcam), anti-rat Hepatocyte Growth Factor (HGF) at 1:200 (Abcam), and anti-rat EGF at 1:200 (Abcam). Secondary antibodies at 1:200 and phalloidin dyes at 1:200 were all AlexaFluor conjugates (Invitrogen). Nuclear stains were used at 1 $\mu$ g/ml for 4',6-diamidino-2-phenylindole (DAPI) (Sigma) and 16.2 $\mu$ M for Hoechst 33342 (Invitrogen).

**Quantification of cell viability.** Cell viability assay was determined using the Live/Dead Viability/Cytotoxicity Kit (Invitrogen). Cells were cultured as described above on PEG-Fibrinogen gels for the indicated time periods, with or without 10ng/ml EGF, or in presence of 10 $\mu$ M cyclic RGD, 10 $\mu$ M mAb225 or cultured on adsorbed collagen I in presence of 10ng/ml EGF. For PEG-Fibrinogen gels, confocal Z-stack images of three to five randomly chosen microwells were taken from each of three to four gels samples per time-point using a 10X objective to capture the entire well (10 micron step size in z-stacks). Total cell number was determined by DAPI staining of nuclei and the number of non-viable cells was determined by ethidium bromide nuclear staining. A total of 200-600 nuclei were counted in each microwell to obtain total cell number. For adsorbed collagen samples, in each transwell, four to six randomly

chosen fields (one from each quadrant of the well) were observed using a 10X objective, and all nuclei were counted in each field (300–600 total nuclei per field). The experiments were performed at least three times (for both PEG-Fibrinogen and adsorbed collagen samples) and data were statistically analyzed with ANOVA followed with Tukey's test with  $\alpha=0.05$ .

**Quantification of albumin and urea production.** Culture medium was replaced 48 hours prior to collection on the indicated days. Albumin levels were determined using Rat Albumin ELISA Kit (Bethyl Labs). Urea levels were determined using the QuantiChrom Urea Assay Kit (BioAssay Systems). Samples, standards and controls were tested in duplicates and experiments were repeated three to six times. Data were normalized to account for sample volumes for both assays. Results are reported as ng Product (urea or albumin) per ml per day in Figure 7. The data were normalized to account for cell number at day of sample collection and are presented as  $\mu\text{g}$  Product (urea or albumin) per  $10^6$  cells per day in Supplemental Figure S5. Cell number per day was calculated based on the total cell counts from the cell viability data for each specific time-point. The data were statistically analyzed with ANOVA followed with Tukey's test with  $\alpha=0.05$ .

**Results:*****Micromolding of PEG-Fibrinogen gels to create a 3-D niche for primary hepatocytes.***

A PEG-Fibrinogen hydrogel formulation was chosen to create niches for primary hepatocytes based on several criteria: amenable to micromolding (in order to isolate small numbers of hepatocytes); intrinsically non-adhesive for hepatocytes, but possessing specific adhesive domains for cell-secreted matrix, to allow interpretation of effects from retention of cell-secreted matrix; physiologically relevant stiffness (similar to liver) should cellular ECM secretion result in adhesion of the cells with the microwell walls. The precise permeability properties of the hydrogel were a secondary consideration, as the cell aggregate itself provides a means of concentrating autocrine factors locally during initial stages of culture, compared to the case of 2D minimally-adhesive surfaces. These criteria were not met by commonly used hydrogels such as collagen and agarose. PEG-Fibrinogen hydrogels met these criteria while providing the additional advantage that secreted fibronectin can interact with fibrinogen subunits within the hydrogel, improving sequestration of cell-derived matrix while only providing adhesion upon autocrine fibronectin retention.

The micromolding scheme is presented in Figure 1, where arrays of microwells filled with 20 $\mu$ m fluorescent beads illustrate the appearance of the wells following final processing steps. The dimensions of the cylindrical features (nominal height,  $h=200\mu\text{m}$ , and nominal diameter,  $d=500\mu\text{m}$ ; actual  $h=213 \pm 19\mu\text{m}$ ,  $d=522 \pm 27\mu\text{m}$ ) were guided by previous studies on the length scales for self-assembly of isolated hepatocytes (confirmed in these studies; data not shown) and diffusion into 3D cultures (44). Bulk elastic moduli of these micromolded hydrogels were measured via atomic force microscopy-enabled indentation ( $E = 17.5 \pm 0.3 \text{ kPa}$  (mean  $\pm$  s.e.m.)), which agrees reasonably well with that reported for liver tissue (33-35). PEG-Fibrinogen hydrogels can be proteolytically degraded, with degradation rates highly dependent

on the content of additional PEG-DA added during polymerization (45). The formulation used here, containing 5% PEG-DA, is in a regime associated with relatively slow degradation, and we saw no evidence of bulk degradation during the course of the experiments.

Primary hepatocytes seeded into microwells in the absence of exogenous EGFR ligands or adhesive matrix molecules aggregated into tissue-like structures over the first 24 hr, formed strong adhesions to the gel matrix, and persisted in tissue-like structures over 10 days of culture (Figure 1B). A modest but noticeable compaction of the tissue structures occurred in the first few days of culture, as expected by increasing cell-cell contacts, causing the structures to pull away from some regions of the walls of the microwells, while remaining firmly attached over about 50% of the contact area. Attempts to culture primary hepatocytes on 2D (non-molded) PEG-Fibrinogen gels were unsuccessful; cells did not attach to the gel, instead forming floating spheroids with little retention of fibronectin, in keeping with previous attempts to culture hepatocytes on fibrinogen (17). Similar results were found with micromolded PEG-DA (Supplemental Figure S1), and agarose gels (data not shown), on which, despite intact features, cells did not attach or persist in microwells, but rather formed viable floating spheroids.

### ***Primary hepatocytes retain cell-derived fibronectin and growth factors within micropatterned wells.***

Hepatocytes lack receptors for fibrinogen. Hence, the observation that primary hepatocytes formed adherent tissue-like structures in the wells of PEG-Fibrinogen gels in the absence of serum or other sources of exogenous ECM or growth factors suggested that the microwells were capable of retaining autocrine factors, including ECM, necessary for cell survival. To determine if primary hepatocytes were able to retain fibronectin matrix and growth factors produced by cells post-isolation, immunofluorescence microscopy was used to monitor the presence of several key autocrine factors produced by hepatocytes.

Fibronectin - ubiquitously present in liver ECM - is assembled from its soluble form into fibrils in an integrin-dependent manner ( $\alpha5\beta1$  in the case of hepatocytes) (46). In culture, thin (5-25 nm) fibrils forming interconnected networks appear in the extracellular environment early in culture, form networks around cells, and mature into thicker fibril bundles at later stages of culture (46). Immunofluorescence staining, as illustrated by confocal imaging of a single slice in the central tissue region, shows the presence of fibronectin in and around primary hepatocytes seeded and cultured in micromolded PEG-Fibrinogen hydrogels, with a staining pattern that suggests formation of fibrils and their maturation over time into fibril bundles (Figure 2). Hepatocytes were cultured as described above, for 3, 7, and 10 days before being fixed, stained with antibodies against fibronectin, and imaged by confocal microscopy to view the region of tissue approximately halfway between the top and bottom of the tissue structure (75-100  $\mu\text{m}$  below the top of the gel). Culture medium was serum-free and did not contain any exogenous matrix molecules or peptide growth factors, except for insulin; hence, observed fibronectin was produced by hepatocytes. Fibronectin with a bright staining pattern characteristic of fibrils is present surrounding cells in the central region of the tissue structures by day 3 and persists at days 7 and 10 (Figure 2, arrows), with a coarsening and thickening of the apparent network by day 10 (Figure 2). In addition to fibrils, diffuse staining is observed within the gel adjacent to the microwell by day 7 (Figure 2). The diffuse appearance of FN staining inside the gel indicates that soluble FN secreted by hepatocytes diffuses into the gel and remains associated with it, as anticipated by the known propensity of FN to associate with regions of fibrinogen. We postulate that interactions between FN and fibrinogen in the gel provide a bridge to link hepatocyte tissue structures firmly to the gel, even as the tissue structures appear to contract slightly and draw away from some regions of the microwell wall at later stages of culture (Figure 2). The gap between the tissue structure and the gel following this slight contraction appears as a dark region between the brightly staining tissue and the diffuse-staining support gel. The

retention of soluble fibronectin within the microwell support structure, and the assembly of fibronectin fibrils within the tissue aggregate are unique to cultures within PEG-Fibrinogen microwells, as cells cultured in PEGDA microwells show diminished fibril assembly within the tissue aggregate and no diffuse staining in the gel wall adjacent to the tissue structure (Figure S1).

The requirement for growth factor signaling, including Hepatocyte Growth Factor (HGF) and EGFR ligands (including EGF and TGF- $\alpha$ ) to maintain primary hepatocyte cultures has been well documented (47-50). The ability of primary hepatocytes to form tissue-like structures on micromolded PEG-Fibrinogen gels in the absence of any of these growth factors provided exogenously implicates autocrine signaling. To examine the presence of autocrine growth factors, primary hepatocytes were cultured in serum-free medium devoid of exogenous growth factors, then fixed and stained with antibodies against EGF, HGF, and TGF- $\alpha$  at days 3, 7, and 10. This protocol detects membrane-bound pro-forms of the growth factors as well as shed factors that become cross-linked to ECM or cell surfaces during fixation. Tissue structures were imaged with low magnification to assess uniformity of stains across multiple wells. All three growth factors are present in the day 3 tissue structures formed by culture of primary adult rat hepatocytes in the microwells (Figure 3) and expression is sustained through days 7 and 10 (Supplemental Figure S2). The apparent lack of staining in the gel adjacent to the tissue structure is not surprising, as growth factors are likely consumed locally in autocrine fashion such that only low (undetectable) concentrations escape into the gel.

***Autocrine matrix and growth factors are necessary and sufficient to maintain the viability of primary hepatocytes in culture.***

The formation and maintenance of tissue-like aggregates of primary hepatocytes within microwells of non-adhesive PEG-Fibrinogen was associated with retention of autocrine factors including fibronectin (Figure 2), EGF, TGF- $\alpha$ , and HGF (Figure 3). Previous studies in 2D culture have shown that survival of primary adult rat hepatocytes is diminished but not abolished in the absence of EGFR ligands (51-53). To determine if autocrine signaling from cell-secreted fibronectin and EGFR ligands is sufficient for cell survival the number and viability of primary adult rat hepatocytes cultured on the PEG-Fibrinogen gels in the absence of serum or exogenous growth factors was measured as a function of time in culture. Total cell numbers were enumerated by counting all nuclei in 3-5 microwells in 3-4 gel samples (at least 200-600 nuclei were counted in each microwell) and non-viable cells were labeled by uptake of ethidium bromide. In micromolded gel substrates, cell number showed a slight (~7%) but statistically insignificant decline over the 10 days of culture, with no statistically significant difference between cultures with or without soluble EGF (Figure 4A). On 2D collagen I-coated substrates in the presence of EGF, a modest (~10%) but statistically significant increase in cell number was observed over 10 days in culture (Figure 4A) consistent with other reports for these culture conditions (29). A similar trend was observed in cell viability during the culture period. Cell viability was assessed by the fraction of cells that excluded ethidium bromide versus total cells stained with DAPI at days 1, 3, 7, and 10. Cells plated on adsorbed collagen I supplemented with EGF exhibit a high level of viability (Figure 4B). Viability of cells in PEG-Fibrinogen cultures was 80-90% with no statistical difference between cultures supplemented with 10 ng/mL EGF and those without. The fate of dead cells was not assessed, and it is possible that cells appearing as non-viable at early time points persist in culture. These data indicate that the autocrine factors present within the microwells are sufficient to sustain hepatocyte viability in long-term culture.

To determine if signaling from either integrin  $\alpha 5\beta 1$  or EGFR is necessary for hepatocyte survival, primary hepatocytes were cultured as described above but in the presence of inhibitors. To block  $\alpha 5\beta 1$ -mediated signaling, cells were cultured with a cyclic RGD peptide to prevent fibronectin and other ECM ligands from binding to this integrin. To block EGFR signaling, cells were cultured in the presence of a monoclonal antibody against EGFR (mAb225) which blocks ligand binding to EGFR, inhibiting autocrine signaling by EGF, TGF- $\alpha$  and any additional autocrine EGFR ligands such as amphiregulin and HB-EGF that may be present. mAb225 binding induces slow internalization and trafficking of EGFR, but does not result in phosphorylation and activation of the EGFR or any known EGFR-mediated signaling events (54). mAb225 was replenished at each medium change to mitigate effects of receptor-mediated down-regulation. The presence of either inhibitor resulted in comparable declines in cell number (Figure 4A) and cell viability (Figure 4B) compared to control cultures. Total cell numbers in the presence of inhibitors on day 1 were ~85% of control values and declined further to ~50% of control values by day 10 (Figure 4A), a trend mirrored by cell viability (Figure 4B). Both inhibitors (i.e., cyclic RGD or EGFR function-blocking antibody) caused a marked decrease in the levels of cell-associated EGF, TGF- $\alpha$ , and HGF as observed by immunofluorescent staining of microwell structures (Supplemental Figure S3). Compared to control cultures, a faint background staining was observed uniformly on the gels for the EGFR-inhibited case, suggesting that cells are still shedding these factors, and in the absence of EGFR uptake, they are adsorbing to the gel-associated ECM. The apparent loss of tissue-associated staining for growth factors in the inhibited cases may be attributed to the decline in cell number due to decreased viability, or due to cross-talk between integrins and growth factors controlling a positive feedback loop of autocrine production, an area for further study.

***Micropatterned PEG-Fibrinogen hydrogels support formation of functional bile canalicular networks.***

*In vivo*, hepatocytes adopt an atypical cell polarity in which the apical cell surface composes the bile canalicular network into which bile is secreted and funneled to the bile duct. To determine the presence of bile canaliculi, cells cultured for 3 days were stained with antibodies to CD26, a marker of the apical surface, and imaged by confocal microscopy. Figures 5A and 5B show a cross-sectional image of a representative tissue-like structure with apical staining at the cell-cell junctions where canaliculi form. Another aspect of this polarity is the presence of fibronectin at the apical surface; unlike other epithelia, hepatocytes lack a canonical basement membrane, instead, fibronectin is found at apical, basal, and lateral surfaces (55). To determine if fibronectin was localizing to the apical surface in addition to the general staining seen in Figure 2, cultures were co-stained with antibodies against fibronectin and CD26. Figures 5C and 5D show that fibronectin does colocalize with CD26 at discrete regions of the apical domain of the hepatocytes. The functionality of the canalicular network was examined using 5 (and 6)-carboxy-2', 7'-dichlorofluorescein diacetate (CDFDA). CDFDA is actively taken up by hepatocytes, de-esterified intracellularly to fluorescent CDF, and secreted into the canaliculi, allowing visualization of canalicular domains with intact tight junctions during a 10-15 minute period before contraction of canaliculi releases their contents into the medium. Results of this assay are shown in Figure 5E, where the CDF is visible in a pattern similar to the CD26 staining. Thus, primary hepatocytes are capable of recapitulating aspects of their complex *in vivo* morphology *in vitro* with only autocrine signals to direct them.

***Autocrine fibronectin is necessary for formation and maintenance of tissue-like structures.***

Fibronectin is abundant in the liver sinusoid where this ECM protein is in direct contact with the hepatocytes that are responsible for production of plasma fibronectin. Similarly, in micromolded PEG-Fibrinogen gels, primary hepatocytes retain fibronectin and create fibrillar networks in the extracellular environment. To determine if this autocrine ECM is crucial for the survival of primary hepatocytes and the formation or maintenance of tissue-like structures, hepatocytes were cultured in the presence of a cyclic RGD peptide that blocks cell-surface  $\alpha 5\beta 1$  integrins from binding fibronectin. Cells were cultured as described above but  $10^{-6}$  M of the cyclic RGD peptide inhibitor was included at the time of plating and subsequent media changes. Cultures were fixed at 3, 7, and 10 days and stained with anti-fibronectin and anti-CD26 antibodies.

Blocking  $\alpha 5\beta 1$  integrin prevents the formation of viable tissue-like aggregates such as those seen in control cultures on day 3, and instead results in dissociated, rounded cells (Figure 6) that gradually become more diffuse by days 7 and 10 (Supplemental Figures S4 and S5) concomitant with significantly reduced viability compared to controls (Figure 4). In control cultures, abundant fibrillar fibronectin networks are observed in the microwells by day 3 (Figure 5 and Figure 6, top), while cultures with the cyclic RGD inhibitor lack detectable extracellular fibronectin, even though intracellular fibronectin is present. Further, cells cultured in the presence of cyclic RGD fail to organize CD26 into canalicular like-structures at early (Figure 6) or late (Figures S4 and S5) stages of culture, instead showing diffuse staining throughout the cell body. The rounded, individual cell morphologies revealed by both FN and CD26 staining show that the cells treated with cyclic RGD have little functional cell-cell contact compared to control cultures. This combined failure to localize CD26 and the absence of extracellular

fibronectin fibrils is in stark contrast to images of control tissue-like aggregates, which show a consistent co-localization of fibronectin fibrils with bile canalicular structures (Figures 5 C and D).

To determine if EGFR signaling was also crucial to the formation or maintenance of the tissue-like structures, hepatocytes were cultured in the presence of the function-blocking EGFR antibody mAb225. The antibody was added to cultures at the time of plating and subsequent media changes, then cells were fixed and stained for FN and CD26 at 3, 7, and 10 days. The tissue structures formed under inhibition of EGFR had a much more compact morphology than controls at day 3, with many dead, dissociated cells in the bottom of the microwell (Figure 6, compare phase and DAPI stains). This highly compact morphology compared to controls (Figure 6) arose from both reduction in cell number by about 40% compared to controls (Figure 4) together with a closer spacing of cells than in the RGD-inhibited case (where cells were partially or completely dissociated), as evidenced by the close location of nuclei in EGFR-inhibited cultures; these patterns were accentuated by day 7 (Supplemental Figure S4) and again by day 10 (Supplemental Figure S5). Interestingly, the total cell numbers and viabilities as a function of time were comparable for both the integrin-inhibited and EGFR-inhibited cultures (Figure 4), yet these cultures had strongly divergent morphologies, with RGD-containing cultures lacking a tissue-like structure (Figures 6, S4 and S5). The pattern of FN and CD26 staining in EGFR-inhibited cultures appears to be predominantly diffuse intracellular (FN) and membrane (CD26) staining (Figures 6, S4 and S5), without the reticular structures seen in controls; bright, condensed regions of staining appear related to the compactness of the culture rather than functional cell-cell contacts, although occasional CD26 reticular structures are seen in the EGFR-inhibited case.

***PEG-Fibrinogen hydrogels promote maintenance of hepatocyte metabolic functions in vitro.*** Primary hepatocytes rapidly dedifferentiate and lose metabolic functions when grown by

standard cell culture techniques, as determined by measuring certain standard metabolic functions of hepatocytes: conversion of ammonia to urea and the production of albumin. Since the PEG-Fibrinogen gels are capable of recapitulating other aspects of hepatocyte function, such as formation of bile canaliculi and production of fibronectin, their metabolic function was monitored and compared to hepatocytes cultured on tissue culture plastic with adsorbed collagen I. Cells were cultured as described above for 10 days and the production of albumin and urea in the conditioned media was assessed. A comparison of the total daily amount of albumin secreted by cells maintained under various culture conditions reveals that at all time-points measured, hepatocytes cultured in the micromolded PEG-Fibrinogen gel format produce statistically greater amounts of albumin compared to cells on adsorbed collagen I (Figure 7 A). Interestingly, minimal to no difference is observed in cultures maintained with or without EGF. The presence of inhibitors of integrin  $\alpha 5\beta 1$  or EGFR function suppress albumin secretion dramatically, to levels <20% of control levels. These trends are further accentuated when albumin production rates (shown in Supplemental Figure S6A) are normalized to viable cell number in Figure 7A. Production of urea follows similar trends across treatment conditions (Figure 7B and Supplemental Figure S6B). These results are in keeping with results presented elsewhere in this report that the retention of autocrine fibronectin and growth factors allow hepatocytes *in vitro* to maintain aspects of their *in vivo* morphology and function.

**Discussion:**

The data presented here implicate autocrine ligands of  $\alpha 5\beta 1$  and EGFR as effectors of hepatocyte function in long-term culture by combining immunostaining illustrating the presence of a subset of known ligands for each receptor type (FN for integrin  $\alpha 5\beta 1$  and TGF- $\alpha$  and EGF for EGFR) with function-blocking inhibitors. In the absence of exogenous adhesion ligands and growth factors, primary hepatocytes cultured in micromolded PEG-Fibrinogen gels are capable of modifying their microenvironment to maintain their differentiation and metabolic function. The PEG-Fibrinogen hydrogel system offered a practical advantage for microwell culture of hepatocytes in that it is not intrinsically adhesive to hepatocytes, which are not known to express receptors for fibrinogen, but can become adhesive in the presence of cell-secreted ECM.

In comparing behavior of hepatocytes seeded onto 2D PEG-Fibrinogen substrates formed by the same gelation process to behavior of cells in microwells, we found that hepatocytes adhered to the gels only when cultured in microwell format. Although hepatocytes did form spheroidal aggregates on the 2D substrates, as they have been observed to do on many minimally adhesive 2D substrates (12, 45), these aggregates failed to adhere to the 2D PEG-Fibrinogen gel substrate. In the microwell format, the local cell environment fosters accumulation of cell-secreted factors simply due to very high local cell density (22) compared to 2D. This phenomenon may be further accentuated if the gel also serves as a diffusion barrier or if it binds factors to provide a local depot for sequestration. The precise permeability properties of these gels were not measured; however, they are expected to be less permeable than PEG-Fibrinogen formulations commonly used for cell encapsulation purposes (36, 39, 40) as they were formed with a relatively high ratio of 6kD PEG-DA (5%) to PEG-Fibrinogen (3.6%). Pure

PEG-DA gels formed with 10-20 kD PEG with 10% polymer content present significant diffusion hindrance to proteins above 20 kD, including HGF, which has a molecular weight ~60 kD (56, 57); small proteins such as EGF likely diffuse relatively unhindered in the as-polymerized gels.

Thus, the differences in formation of adherent cell aggregates during the first day of culture in the microwell format compared to 2D culture on the same substrate may arise from higher local concentration of small peptide factors such as EGF, due to locally high cell concentrations in microwells compared to 2D. These effects may be coupled with enhanced retention of larger autocrine factors such as HGF and enhanced local concentrations of fibronectin due to reduced permeability of the gel to large proteins. Another factor that may be operative in early stages to facilitate interactions between ECM and the gel in microwell format compared to 2D is attainment of locally high concentrations of proteases. Extracellular proteases may degrade the gel to increase the surface area for gel-ECM interaction in the microwell compared to 2D format. Secreted proteases range in size from about 20kD to over 100 kD, hence, a substantial fraction of proteases would likely exhibit hindered diffusion in the gel compared to culture medium. As reported previously (36), PEG-Fibrinogen gels polymerized with high additional PEG-DA macromer content exhibit relatively slow enzymatic degradation compared to pure PEG-Fibrinogen gels, but even a modest degree of local remodeling may enhance adhesion of ECM and cells. Although other types of cells encapsulated in or cultured on PEG-Fibrinogen gels have been observed to migrate into gels, we did not observe cellular in-growth into the gels or observe any signs of bulk gel degradation (e.g. swelling or fracturing of the gels) for cells cultured in the microwell format. Adult hepatocytes are not highly migratory (13) and proteases tend to act in a highly local fashion, hence we would not anticipate, nor did we observe, bulk gel degradation for a format where cells are so highly localized.

Previous work has found a role for fibronectin in a variety of developmental, regenerative and disease processes in the liver. For example, during regeneration after partial hepatectomy, there are elevated levels of fibronectin and  $\alpha 5$  and  $\beta 1$  integrin subunits, and decreased levels of gap junctions in the plasma membrane of hepatocytes prior to and during regeneration (58). Our work here, supports that role, as a blockade of  $\alpha 5 \beta 1$  hinders viability of hepatocytes. It is also interesting to speculate if this increase in cell-matrix adhesions coincidental to a decrease in cell-cell adhesions during regeneration explains the ability of the cyclic RGD peptide to inhibit formation of tissue-like aggregates as we find that bile canaliculi fail to form in the absence of fibronectin fibrils and  $\alpha 5 \beta 1$  signaling (Figure 6, S4, S5). *In vivo*, fibronectin is observed at all hepatocyte plasma membrane domains: sinusoidal, lateral, and apical/canalicular (55, 58, 59). However, during development and oncogenesis, the distribution of the non-integrin fibronectin receptor AGp110 correlates with the differentiation state of hepatocytes; AGp110 localization at the apical (canalicular) membrane indicates a differentiated state (60-62). Hence, the loss of metabolic function in the absence of FN fibril formation and  $\alpha 5 \beta 1$  signaling may be due to dedifferentiation resulting from the lack of cell polarity. It is also possible that more generalized signals from fibronectin are crucial to the survival and differentiation of hepatocytes, without which, the cells dedifferentiate and are rendered incapable of maintaining cell-cell contacts and other functions.

Growth factors also play a crucial role in liver development and regeneration, notably, HGF (ligand for c-MET), and EGFR ligands, including TGF- $\alpha$ , and EGF. The relationship between these growth factors is complex, with a high level of redundancy amongst EGFR ligands as well as synergy with other growth factor receptors (63, 64). For instance, mouse knockouts of TGF- $\alpha$  or of EGF show no impairment of liver development and loss of TGF- $\alpha$  does not impair liver regeneration. However, loss of EGFR – the signaling nexus for multiple extracellular ligands -

causes impairment of liver regeneration in some models (65, 66), though not others (67, 68), where conflicting results may be attributed to differences in species, strain, and the specificity of silencing EGFR in hepatocytes. Although the effects of EGFR ablation on regeneration are equivocal, loss of c-MET, the receptor for HGF, dramatically impairs both embryonic development and liver regeneration (65, 69). In cultures where EGFR autocrine stimulation was blocked by mAb225, we observed a very significant loss of viability compared to control cultures (Figures 4A and 4B), thus, *in vitro*, it appears that c-MET stimulation by autocrine HGF (Figure 4 and S3) does not completely compensate for the loss of EGFR signaling.

Determining the role of individual autocrine growth factors is further complicated by the potential for synergy or cooperativity with integrins. In a variety of cell types, it has been shown that integrin ligand binding and clustering result in increased growth factor receptor phosphorylation and enhanced signaling in shared downstream pathways (70-73). In light of these facts, it is not surprising that hepatocytes in micromolded PEG-Fibrinogen cultures require both integrin as well as growth factor signaling for proper survival and morphology as well as maintenance of differentiated metabolic functions. This system may be useful in further dissecting the intersecting and overlapping pathways between integrin and growth factor receptors that constitute the autocrine signaling network in the liver.

**Conclusion:**

Autocrine matrix and growth factor regulation of primary rat hepatocyte survival and function in the absence of exogenous growth factors and adhesive ligands was studied using micropatterned PEG-Fibrinogen hydrogels to provide an appropriate environment for 3D culture. Retention of autocrine-generated fibronectin, TGF- $\alpha$ , EGF, and HGF by hepatocytes was observed in these 3D cultures, which assumed a tissue-like appearance and developed attachment to the walls of the microwells. Hepatocytes cultured in microwells adopted complex polarity including a functional bile canaliculi-like network, and maintained their viability and production of urea and albumin. Inhibition of  $\alpha 5\beta 1$  integrin binding to fibronectin and inhibition of EGFR signaling in this culture format resulted in decreased hepatocyte survival and metabolic function and a decrease in soluble TGF- $\alpha$ , HGF and EGF sequestration in the 3D tissue structure. Further, inhibition of  $\alpha 5\beta 1$  integrin showed a deficiency in fibrillar fibronectin assembly, a disruption in the formation of tissue-like aggregates, and a failure of cells to polarize. Thus, this report indicates that autocrine matrix and growth factors are necessary and sufficient for maintenance of hepatocyte differentiation and survival *in vitro*.

---

## Acknowledgements

We appreciate the careful reading of the manuscript by and thoughtful discussions with Prof. Roger D. Kamm (MIT). We thank Linda Stockdale (Griffith lab) for synthesizing PEG-DA and Karel Domansky (Biotechnology Process Engineering Center, MIT) for provision of polycarbonate scaffolds. We are thankful to Rachel Pothier (Griffith lab) for provision of primary hepatocytes. We thank Tracey Allen (UROP student, Griffith lab) for help with albumin and urea assays. A. Zeiger acknowledges generous support by the US National Science & Engineering Defense Graduate Fellowship. We are also grateful to Vernella Vickerman and Seok Chung (Kamm lab) for silicon master mold. We acknowledge funding from the National Institutes of Health (NIBIB R01EB003805 (LGG); NIEHS, through the MIT Center for Environmental Health Sciences P30ES002109 (LGG), and R01ES015241 (LGG), and an NRSA postdoctoral fellowship to SRP) and National Science Foundation CAREER Award (KVV).

## Author Disclosure Statement

No competing financial interests exist.

## References:

1. Michalopoulos, G.K. Liver regeneration. *J Cell Physiol* 213, 286, 2007.
2. Weiner, O.H., Zoremba, M., and Gressner, A.M. Gene expression of syndecans and betaglycan in isolated rat liver cells. *Cell Tissue Res* 285, 11, 1996.
3. Martinez-Hernandez, A. The hepatic extracellular matrix. I. Electron immunohistochemical studies in normal rat liver. *Lab Invest* 51, 57, 1984.
4. De Smet, K., Beken, S., Depreter, M., Roels, F., Vercruysse, A., and Rogiers, V. Effect of Epidermal Growth Factor in Collagen Gel Cultures of Rat Hepatocytes. *Toxicology in vitro* 13, 579, 1999.
5. Fremin, C., Bessard, A., Ezan, F., Gailhouste, L., Regeard, M., Le Seyec, J., Gilot, D., Pages, G., Pouyssegur, J., Langouet, S., and Baffet, G. Multiple division cycles and long-term survival of hepatocytes are distinctly regulated by extracellular signal-regulated kinases ERK1 and ERK2. *Hepatology* 49, 930, 2009.
6. Iocca, H.A., and Isom, H.C. Tumor necrosis factor-alpha acts as a complete mitogen for primary rat hepatocytes. *Am J Pathol* 163, 465, 2003.
7. Kim, S.H., and Akaike, T. Epidermal growth factor signaling for matrix-dependent cell proliferation and differentiation in primary cultured hepatocytes. *Tissue Eng* 13, 601, 2007.
8. McGowan, J.A., Strain, A.J., and Bucher, N.L. DNA synthesis in primary cultures of adult rat hepatocytes in a defined medium: effects of epidermal growth factor, insulin, glucagon, and cyclic-AMP. *J Cell Physiol* 108, 353, 1981.
9. Okamoto, H., Kimura, M., Watanabe, N., and Ogihara, M. Tumor necrosis factor (TNF) receptor-2-mediated DNA synthesis and proliferation in primary cultures of adult rat hepatocytes: The involvement of endogenous transforming growth factor-alpha. *Eur J Pharmacol* 604, 12, 2009.
10. Brophy, C.M., Luebke-Wheeler, J.L., Amiot, B.P., Khan, H., Rimmel, R.P., Rinaldo, P., and Nyberg, S.L. Rat hepatocyte spheroids formed by rocked technique maintain differentiated hepatocyte gene expression and function. *Hepatology* 49, 578, 2009.
11. Kawaguchi, M., Koide, N., Sakaguchi, K., Shinji, T., and Tsuji, T. Combination of epidermal growth factor and insulin is required for multicellular spheroid formation of rat hepatocytes in primary culture. *Acta Med Okayama* 46, 195, 1992.
12. Koide, N., Sakaguchi, K., Koide, Y., Asano, K., Kawaguchi, M., Matsushima, H., Takenami, T., Shinji, T., Mori, M., and Tsuji, T. Formation of multicellular spheroids composed of adult rat hepatocytes in dishes with positively charged surfaces and under other nonadherent environments. *Exp Cell Res* 186, 227, 1990.
13. Powers, M.J., Rodriguez, R.E., and Griffith, L.G. Cell-substratum adhesion strength as a determinant of hepatocyte aggregate morphology. *Biotechnol Bioeng* 53, 415, 1997.
14. Koide, N., Shinji, T., Tanabe, T., Asano, K., Kawaguchi, M., Sakaguchi, K., Koide, Y., Mori, M., and Tsuji, T. Continued high albumin production by multicellular spheroids of adult rat hepatocytes formed in the presence of liver-derived proteoglycans. *Biochem Biophys Res Commun* 161, 385, 1989.
15. Riccalton-Banks, L., Liew, C., Bhandari, R., Fry, J., and Shakesheff, K. Long-term culture of functional liver tissue: three-dimensional coculture of primary hepatocytes and stellate cells. *Tissue Eng* 9, 401, 2003.
16. Shinji, T., Koide, N., and Tsuji, T. Glycosaminoglycans partially substitute for proteoglycans in spheroid formation of adult rat hepatocytes in primary culture. *Cell Struct Funct* 13, 179, 1988.
17. Stamatoglou, S.C., Hughes, R.C., and Lindahl, U. Rat hepatocytes in serum-free primary culture elaborate an extensive extracellular matrix containing fibrin and fibronectin. *J Cell Biol* 105, 2417, 1987.

18. Tong, J.Z., De Lagausie, P., Furlan, V., Cresteil, T., Bernard, O., and Alvarez, F. Long-term culture of adult rat hepatocyte spheroids. *Exp Cell Res* 200, 326, 1992.
19. Tostoes, R.M., Leite, S.B., Miranda, J.P., Sousa, M., Carrondo, M.J., and Alves, P.M. Perfusion of 3D encapsulated hepatocytes - a synergistic effect enhancing long term functionality in bioreactors. *Biotechnol Bioeng*, 2010.
20. Sivaraman, A., Leach, J.K., Townsend, S., Iida, T., Hogan, B.J., Stolz, D.B., Fry, R., Samson, L.D., Tannenbaum, S.R., and Griffith, L.G. A microscale in vitro physiological model of the liver: predictive screens for drug metabolism and enzyme induction. *Curr Drug Metab* 6, 569, 2005.
21. Cosgrove, B.D., Cheng, C., Pritchard, J.R., Stolz, D.B., Lauffenburger, D.A., and Griffith, L.G. An inducible autocrine cascade regulates rat hepatocyte proliferation and apoptosis responses to tumor necrosis factor-alpha. *Hepatology* 48, 276, 2008.
22. DeWitt, A., Iida, T., Lam, H.Y., Hill, V., Wiley, H.S., and Lauffenburger, D.A. Affinity regulates spatial range of EGF receptor autocrine ligand binding. *Dev Biol* 250, 305, 2002.
23. Dvir-Ginzberg, M., Elkayam, T., Aflalo, E.D., Agbaria, R., and Cohen, S. Ultrastructural and functional investigations of adult hepatocyte spheroids during in vitro cultivation. *Tissue Eng* 10, 1806, 2004.
24. Peshwa, M.V., Wu, F.J., Sharp, H.L., Cerra, F.B., and Hu, W.S. Mechanistic of formation and ultrastructural evaluation of hepatocyte spheroids. *In Vitro Cell Dev Biol Anim* 32, 197, 1996.
25. Fassett, J., Tobolt, D., and Hansen, L.K. Type I collagen structure regulates cell morphology and EGF signaling in primary rat hepatocytes through cAMP-dependent protein kinase A. *Mol Biol Cell* 17, 345, 2006.
26. Nelson, C.M., Vanduijn, M.M., Inman, J.L., Fletcher, D.A., and Bissell, M.J. Tissue geometry determines sites of mammary branching morphogenesis in organotypic cultures. *Science* 314, 298, 2006.
27. Okochi, N., Okazaki, T., and Hattori, H. Encouraging effect of cadherin-mediated cell-cell junctions on transfer printing of micropatterned vascular endothelial cells. *Langmuir* 25, 6947, 2009.
28. Raghavan, S., Nelson, C.M., Baranski, J.D., Lim, E., and Chen, C.S. Geometrically Controlled Endothelial Tubulogenesis in Micropatterned Gels. *Tissue Eng Part A*, 2010.
29. Mehta, G., Williams, C.M., Alvarez, L., Lesniewski, M., Kamm, R.D., and Griffith, L.G. Synergistic effects of tethered growth factors and adhesion ligands on DNA synthesis and function of primary hepatocytes cultured on soft synthetic hydrogels. *Biomaterials* 31, 4657, 2010.
30. Scheving, L.A., Zhang, L., Stevenson, M.C., Kwak, E.S., and Russell, W.E. The emergence of ErbB2 expression in cultured rat hepatocytes correlates with enhanced and diversified EGF-mediated signaling. *Am J Physiol Gastrointest Liver Physiol* 291, G16, 2006.
31. Makogonenko, E., Tsurupa, G., Ingham, K., and Medved, L. Interaction of fibrin(ogen) with fibronectin: further characterization and localization of the fibronectin-binding site. *Biochemistry* 41, 7907, 2002.
32. Frisman, I., Orbach, R., Seliktar, D., and Bianco-Peled, H. Structural investigation of PEG-fibrinogen conjugates. *J Mater Sci Mater Med* 21, 73, 2010.
33. Arena, U., Vizzutti, F., Corti, G., Ambu, S., Stasi, C., Bresci, S., Moscarella, S., Boddi, V., Petrarca, A., Laffi, G., Marra, F., and Pinzani, M. Acute viral hepatitis increases liver stiffness values measured by transient elastography. *Hepatology* 47, 380, 2008.
34. Corpechot, C., El Naggar, A., Poujol-Robert, A., Ziol, M., Wendum, D., Chazouilleres, O., de Ledinghen, V., Dhumeaux, D., Marcellin, P., Beaugrand, M., and Poupon, R. Assessment of biliary fibrosis by transient elastography in patients with PBC and PSC. *Hepatology* 43, 1118, 2006.

35. Ganne-Carrie, N., Ziolo, M., de Ledinghen, V., Douvin, C., Marcellin, P., Castera, L., Dhumeaux, D., Trinchet, J.C., and Beaugrand, M. Accuracy of liver stiffness measurement for the diagnosis of cirrhosis in patients with chronic liver diseases. *Hepatology* 44, 1511, 2006.
36. Dikovsky, D., Bianco-Peled, H., and Seliktar, D. The effect of structural alterations of PEG-fibrinogen hydrogel scaffolds on 3-D cellular morphology and cellular migration. *Biomaterials* 27, 1496, 2006.
37. Hwa, A.J., Fry, R.C., Sivaraman, A., So, P.T., Samson, L.D., Stolz, D.B., and Griffith, L.G. Rat liver sinusoidal endothelial cells survive without exogenous VEGF in 3D perfused co-cultures with hepatocytes. *Faseb J* 21, 2564, 2007.
38. Hern, D.L., and Hubbell, J.A. Incorporation of adhesion peptides into nonadhesive hydrogels useful for tissue resurfacing. *J Biomed Mater Res* 39, 266, 1998.
39. Peyton, S.R., Kim, P.D., Ghajar, C.M., Seliktar, D., and Putnam, A.J. The effects of matrix stiffness and RhoA on the phenotypic plasticity of smooth muscle cells in a 3-D biosynthetic hydrogel system. *Biomaterials* 29, 2597, 2008.
40. Almany, L., and Seliktar, D. Biosynthetic hydrogel scaffolds made from fibrinogen and polyethylene glycol for 3D cell cultures. *Biomaterials* 26, 2467, 2005.
41. Domansky, K., Inman, W., Serdy, J., Dash, A., Lim, M.H., and Griffith, L.G. Perfused multiwell plate for 3D liver tissue engineering. *Lab Chip* 10, 51, 2010.
42. Maloney, J.M., Walton, E.B., Bruce, C.M., and Van Vliet, K.J. Influence of finite thickness and stiffness on cellular adhesion-induced deformation of compliant substrata. *Phys Rev E Stat Nonlin Soft Matter Phys* 78, 041923, 2008.
43. Thompson, M.T., Berg, M.C., Tobias, I.S., Rubner, M.F., and Van Vliet, K.J. Tuning compliance of polyelectrolyte multilayers to modulate cell adhesion. *Biomaterials* 26, 6836, 2005.
44. Powers, M.J., Domansky, K., Kaazempur-Mofrad, M.R., Kalezi, A., Capitano, A., Upadhyaya, A., Kurzawski, P., Wack, K.E., Stolz, D.B., Kamm, R., and Griffith, L.G. A microfabricated array bioreactor for perfused 3D liver culture. *Biotechnol Bioeng* 78, 257, 2002.
45. Dikovsky, D., Bianco-Peled, H., and Seliktar, D. Defining the role of matrix compliance and proteolysis in three-dimensional cell spreading and remodeling. *Biophys J* 94, 2914, 2008.
46. Singh, P., Carraher, C., and Schwarzbauer, J.E. Assembly of fibronectin extracellular matrix. *Annu Rev Cell Dev Biol* 26, 397, 2010.
47. Block, G.D., Locker, J., Bowen, W.C., Petersen, B.E., Katyal, S., Strom, S.C., Riley, T., Howard, T.A., and Michalopoulos, G.K. Population expansion, clonal growth, and specific differentiation patterns in primary cultures of hepatocytes induced by HGF/SF, EGF and TGF alpha in a chemically defined (HGM) medium. *J Cell Biol* 132, 1133, 1996.
48. Michalopoulos, G.K., Bowen, W., Nussler, A.K., Becich, M.J., and Howard, T.A. Comparative analysis of mitogenic and morphogenic effects of HGF and EGF on rat and human hepatocytes maintained in collagen gels. *J Cell Physiol* 156, 443, 1993.
49. Michalopoulos, G.K., Bowen, W.C., Mule, K., and Luo, J. HGF-, EGF-, and dexamethasone-induced gene expression patterns during formation of tissue in hepatic organoid cultures. *Gene Expr* 11, 55, 2003.
50. Tomiya, T., Omata, M., Imamura, H., and Fujiwara, K. Impaired liver regeneration in acute liver failure: the significance of cross-communication of growth associated factors in liver regeneration. *Hepatol Res* 38, S29, 2008.
51. De Smet, K., Loyer, P., Gilot, D., Vercruyse, A., Rogiers, V., and Guguen-Guillouzo, C. Effects of epidermal growth factor on CYP inducibility by xenobiotics, DNA replication, and caspase activations in collagen I gel sandwich cultures of rat hepatocytes. *Biochem Pharmacol* 61, 1293, 2001.
52. Jansing, R., and Samsonoff, W.A. Effect of epidermal growth factor on cultured adult rat hepatocytes. *Tissue Cell* 16, 157, 1984.
53. Serra, R., and Isom, H.C. Stimulation of DNA synthesis and protooncogene expression in primary rat hepatocytes in long-term DMSO culture. *J Cell Physiol* 154, 543, 1993.

54. Liao, H.J., and Carpenter, G. Cetuximab/C225-induced intracellular trafficking of epidermal growth factor receptor. *Cancer Res* 69, 6179, 2009.
55. Enrich, C., Evans, W.H., and Gahmberg, C.G. Fibronectin isoforms in plasma membrane domains of normal and regenerating rat liver. *FEBS Lett* 228, 135, 1988.
56. Cruise, G.M., Scharp, D.S., and Hubbell, J.A. Characterization of permeability and network structure of interfacially photopolymerized poly(ethylene glycol) diacrylate hydrogels. *Biomaterials* 19, 1287, 1998.
57. Weber, L.M., Lopez, C.G., and Anseth, K.S. Effects of PEG hydrogel crosslinking density on protein diffusion and encapsulated islet survival and function. *J Biomed Mater Res A* 90, 720, 2009.
58. Pujades, C., Forsberg, E., Enrich, C., and Johansson, S. Changes in cell surface expression of fibronectin and fibronectin receptor during liver regeneration. *J Cell Sci* 102 ( Pt 4), 815, 1992.
59. Hughes, R.C., and Stamatoglou, S.C. Adhesive interactions and the metabolic activity of hepatocytes. *J Cell Sci Suppl* 8, 273, 1987.
60. Stamatoglou, S.C., Enrich, C., Manson, M.M., and Hughes, R.C. Temporal changes in the expression and distribution of adhesion molecules during liver development and regeneration. *J Cell Biol* 116, 1507, 1992.
61. Stamatoglou, S.C., Manson, M.M., Green, J.A., Mayol, X., and Hughes, R.C. Distribution of fibronectin and fibronectin-binding proteins, AGp110 and integrin alpha 5 beta 1, during chemically induced hepatocarcinogenesis in adult rats. *J Cell Sci* 100 ( Pt 3), 599, 1991.
62. Torbenson, M., Wang, J., Choti, M., Ashfaq, R., Maitra, A., Wilentz, R.E., and Boitnott, J. Hepatocellular carcinomas show abnormal expression of fibronectin protein. *Mod Pathol* 15, 826, 2002.
63. Scheving, L.A., Stevenson, M.C., Taylormoore, J.M., Traxler, P., and Russell, W.E. Integral role of the EGF receptor in HGF-mediated hepatocyte proliferation. *Biochem Biophys Res Commun* 290, 197, 2002.
64. Stolz, D.B., and Michalopoulos, G.K. Comparative effects of hepatocyte growth factor and epidermal growth factor on motility, morphology, mitogenesis, and signal transduction of primary rat hepatocytes. *J Cell Biochem* 55, 445, 1994.
65. Natarajan, A., Wagner, B., and Sibilias, M. The EGF receptor is required for efficient liver regeneration. *Proc Natl Acad Sci U S A* 104, 17081, 2007.
66. Skarpen, E., Oksvold, M.P., Grosvik, H., Widnes, C., and Huitfeldt, H.S. Altered regulation of EGF receptor signaling following a partial hepatectomy. *J Cell Physiol* 202, 707, 2005.
67. Paranjpe, S., Bowen, W.C., Tseng, G.C., Luo, J.H., Orr, A., and Michalopoulos, G.K. RNA interference against hepatic epidermal growth factor receptor has suppressive effects on liver regeneration in rats. *Am J Pathol* 176, 2669, 2010.
68. Van Buren, G., 2nd, Yang, A.D., Dallas, N.A., Gray, M.J., Lim, S.J., Xia, L., Fan, F., Somcio, R., Wu, Y., Hicklin, D.J., and Ellis, L.M. Effect of molecular therapeutics on liver regeneration in a murine model. *J Clin Oncol* 26, 1836, 2008.
69. Schmidt, C., Bladt, F., Goedecke, S., Brinkmann, V., Zschiesche, W., Sharpe, M., Gherardi, E., and Birchmeier, C. Scatter factor/hepatocyte growth factor is essential for liver development. *Nature* 373, 699, 1995.
70. Cabodi, S., Moro, L., Bergatto, E., Boeri Erba, E., Di Stefano, P., Turco, E., Tarone, G., and Defilippi, P. Integrin regulation of epidermal growth factor (EGF) receptor and of EGF-dependent responses. *Biochem Soc Trans* 32, 438, 2004.
71. Lee, J.W., and Juliano, R.L. The alpha5beta1 integrin selectively enhances epidermal growth factor signaling to the phosphatidylinositol-3-kinase/Akt pathway in intestinal epithelial cells. *Biochim Biophys Acta* 1542, 23, 2002.

- 
72. Miyamoto, S., Teramoto, H., Gutkind, J.S., and Yamada, K.M. Integrins can collaborate with growth factors for phosphorylation of receptor tyrosine kinases and MAP kinase activation: roles of integrin aggregation and occupancy of receptors. *J Cell Biol* 135, 1633, 1996.
73. Moro, L., Venturino, M., Bozzo, C., Silengo, L., Altruda, F., Beguinot, L., Tarone, G., and Defilippi, P. Integrins induce activation of EGF receptor: role in MAP kinase induction and adhesion-dependent cell survival. *Embo J* 17, 6622, 1998.

## List of Figures:

**Figure 1: Micromolding of PEG-Fibrinogen hydrogels.** **A.** PEG-Fibrinogen gels were polymerized as described in Supplementary Information (Materials and Methods) on top of a polycarbonate support scaffold visible by phase microscopy. After polymerization, fluorescent microbeads were placed on the patterned gel and sonicated for 30 seconds to allow the beads to settle inside the negative features of the PEG-Fibrinogen gel. The gel was subsequently washed with PBS to remove floating beads and imaged by fluorescence microscopy. Microwells filled with beads are indicated by arrow, support scaffold channels are indicated by arrowhead. For reference, the microbeads are  $d=20\mu\text{m}$  and support scaffold channels are  $d=340\mu\text{m}$ . Scale bar = 1mm. **B.** Freshly isolated primary hepatocytes were plated onto molded gels, as described in Supplementary Information (Materials and Methods), at a density of 100,000 cells/cm<sup>2</sup> (720,000 cells/ml) in hepatocyte growth medium lacking growth factors (except for insulin). Three days after plating, cultures were fixed and stained to label the nuclei (blue) and the actin cytoskeleton (orange). Single confocal cross-sections taken within the centermost 25% of the structure are shown. Scale bar = 100 $\mu\text{m}$ .

## Figure 2: Primary hepatocytes retain fibronectin matrix within micropatterned wells.

Primary hepatocytes were plated as previously described. At 3, 7, and 10 days, cells were fixed and stained for fibronectin (green) and nuclei (blue). Confocal images were taken at 20X and digital zoom of red highlighted regions is illustrated in top right insets. Single confocal cross-sections taken within the centermost 25% of the structure are depicted. Note intracellular fibronectin (arrowheads), fibronectin fibrils (arrows) and staining for secreted, soluble fibronectin trapped in the walls of the microwell (open arrowheads). (For phase images see Figures 1 and 6 (day 3), Figure S4 (day 7) and Figure S5 (day10). Scale bar = 100  $\mu\text{m}$ .)

**Figure 3: Primary hepatocytes retain autocrine growth factors in micropatterned wells.**

Cells were cultured as previously described, in the absence of serum or exogenous growth factors (except for insulin). After three days, samples were fixed and stained with antibodies against EGF, HGF, and TGF- $\alpha$ . As a negative control, a sample was incubated with secondary antibody alone to confirm that signal was from primary antibody. Fluorescence indicates retention of TGF- $\alpha$ , EGF, and HGF. Microwells filled with cells are indicated by arrow, support scaffold channels are indicated arrowhead. Support scaffold channels are  $d=340\ \mu\text{m}$ , scale bar = 1mm (Magnification 35 X). For days 7 and 10, see Supplemental Figure S2.

**Figure 4: Autocrine signaling is necessary and sufficient for the survival of primary**

**hepatocytes *in vitro*.** **A)** Total cell numbers as a function of time in culture, **B)** Quantification of cell viability expressed as percentage of viable cells. Freshly isolated primary hepatocytes were plated onto molded gels at a density of 100,000 cells/cm<sup>2</sup> in hepatocyte growth medium with 10ng/ml EGF (white, sEGF), no EGF (dark grey, no EGF), no EGF with 10 $\mu\text{M}$  cyclic RGD peptide (light grey, cRGD), or no EGF with 10 $\mu\text{M}$  mAb225 (black, mAb225). Hepatocytes were cultured on adsorbed collagen I at a density of 100,000 cells/cm<sup>2</sup> in hepatocyte growth medium supplemented with 10ng/ml EGF (diagonal pattern, Ads Col I). At the indicated time-points, viable cells were identified by their ability to exclude Ethidium Bromide and total cell numbers were determined with DAPI staining. The horizontal lines depict total number of cells seeded on PEG-Fibrinogen gels and adsorbed collagen substrates. For PEG-Fibrinogen gels, total number of cells effectively seeded into 35 microwells per culture is based on measurements of the number of nuclei in 20 microwells in 4 samples 24 hr after plating. \* indicates statistical significance as compared to PEG gel soluble EGF condition on that specific day,  $p<0.05$ ,  $n>3$ .

**Figure 5: Micropatterned PEG-Fibrinogen hydrogels support 3D polarization of primary hepatocytes and the formation of a functional bile canalicular network.** Cells were plated and cultured in hepatocyte growth medium without EGF as previously described, then fixed and stained for the indicated epitopes. Single confocal cross-sections taken within the centermost 25% of the structure are depicted. **A** and **B**, Cells cultured for 3 days and stained for CD26 (green), nuclei (blue), and the actin cytoskeleton (orange), samples imaged at 10X (**A**) and 63X (**B**). **C** and **D**, Cells cultured for 7 days and stained for CD26 (orange), fibronectin (green), and nuclei (blue), samples imaged at 20X (**C**) and 40X (**D**). **E**, Visualization of functional bile canaliculi by confocal microscopy on day 6 using 5 (and 6)-carboxy-2',7'-dichlorofluorescein (CDF) diacetate at 20X (with digital zoom of red highlighted region in top right inset). For reference, support scaffold channels are  $d=340\ \mu\text{m}$ . Scale bar =  $50\ \mu\text{m}$  in each image. Note regions of plasma membrane showing CD26 and fibronectin colocalization (arrows), and concentrated CDF staining in the 3-D tissue structure, which is similar to CD26 staining in **5A** and **5B** (arrowheads = bile canaliculi, dotted arrows = intracellular uptake of CDF).

**Figure 6: Blocking  $\alpha 5\beta 1$  but not EGFR disrupts tissue-like structures.** Cells were plated as described above and cultured for 3 days in the absence or presence of  $10\ \mu\text{M}$  cyclic RGD peptide or mAb225. After 3 days, cultures were fixed and stained for fibronectin (green), CD26 (orange), and nuclei (blue). Note the absence of fibronectin fibrils or discrete CD26 staining and the loose, dissociated cells in the microwells of cultures with cyclic RGD. Also note the smooth edges of the aggregates, loose cells in the bottom of the well, and staining for fibronectin and CD26 similar to control culture in the microwells of cultures with mAb225. For reference, support scaffold channels are  $d=340\ \mu\text{m}$ . Scale bar =  $100\ \mu\text{m}$ . For days 7 and 10, see Supplementary Figures S4 and S5.

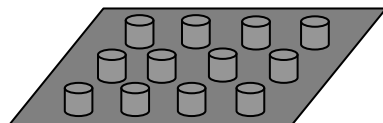
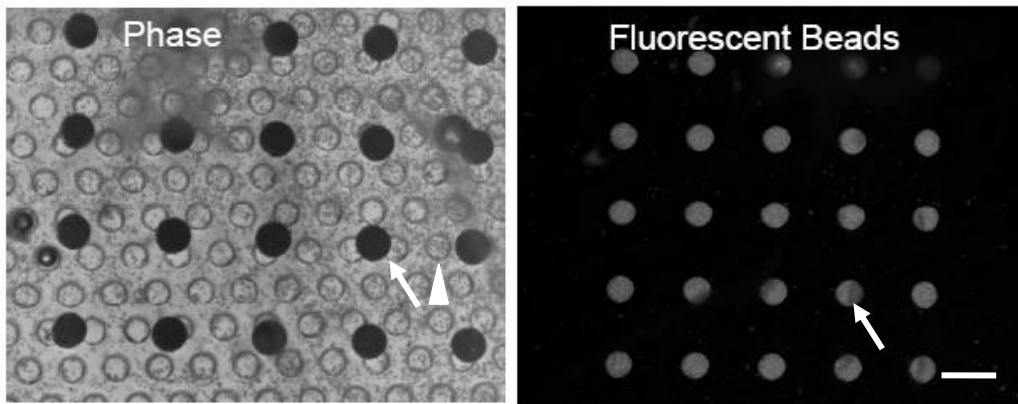
**Figure 7: PEG-Fibrinogen hydrogels promote maintenance of hepatocyte metabolic functions *in vitro*.** Primary hepatocytes were cultured on micromolded PEG-Fibrinogen gels or adsorbed collagen I as described in Materials and Methods. Conditioned medium was collected at the indicated time-points and metabolites of interest were quantified as described in Materials and Methods. Samples, standards, and controls were tested in duplicate. **A)** Albumin synthesis, **B)** Urea synthesis. \*indicates statistically significant difference from sEGF supplemented PEG-Fibrinogen samples at a specific day,  $p < 0.05$ ,  $n > 3$ . For absolute (non-normalized) rates of secretion, see Supplementary Figure S6.

**Reprint Author:**

Linda G. Griffith  
 S.E.T.I. Professor of Mechanical and Biological Engineering  
 Director of Biotechnology Process Engineering Center (BPEC)  
 Massachusetts Institute of Technology  
 77 Massachusetts Avenue, 16-429,  
 Cambridge, MA, 02139-4307, USA

Email: griff@mit.edu  
 Phone: +1 617 253 0013  
 Fax: +1 617 253 2400

**Tissue Engineering Manuscript ID TEA-2010-0398: Autocrine-controlled formation and function of tissue-like aggregates by primary hepatocytes in micropatterned hydrogel arrays**

**Figures:**

PDMS mold  
 Cylindrical features  
 $h=200\ \mu\text{m}$ ,  $d=500\ \mu\text{m}$

**A****B**

**Figure 1: Micromolding of PEG-Fibrinogen hydrogels.** **A.** PEG-Fibrinogen gels were polymerized as described in Supplementary Information (Materials and Methods) on top of a polycarbonate support scaffold visible by phase microscopy. After polymerization, fluorescent microbeads were placed on the patterned gel and sonicated for 30 seconds to allow the beads to settle inside the negative features of the PEG-Fibrinogen gel. The gel was subsequently washed with PBS to remove floating beads and imaged by fluorescence microscopy. Microwells filled with beads are indicated by arrow, support scaffold channels are indicated arrowhead. For reference, the microbeads are  $d=20\mu\text{m}$  and support scaffold channels are  $d=340\mu\text{m}$ . Scale bar = 1mm. **B.** Freshly isolated primary hepatocytes were plated onto molded gels, as described in Supplementary Information (Materials and Methods), at a density of 100,000 cells/cm<sup>2</sup> (720,000 cells/ml) in hepatocyte growth medium lacking growth factors (except for insulin). Three days after plating, cultures were fixed and stained to label the nuclei (blue) and the actin cytoskeleton (orange). Single confocal cross-sections taken within the centermost 25% of the structure are shown. Scale bar = 100 $\mu\text{m}$ .

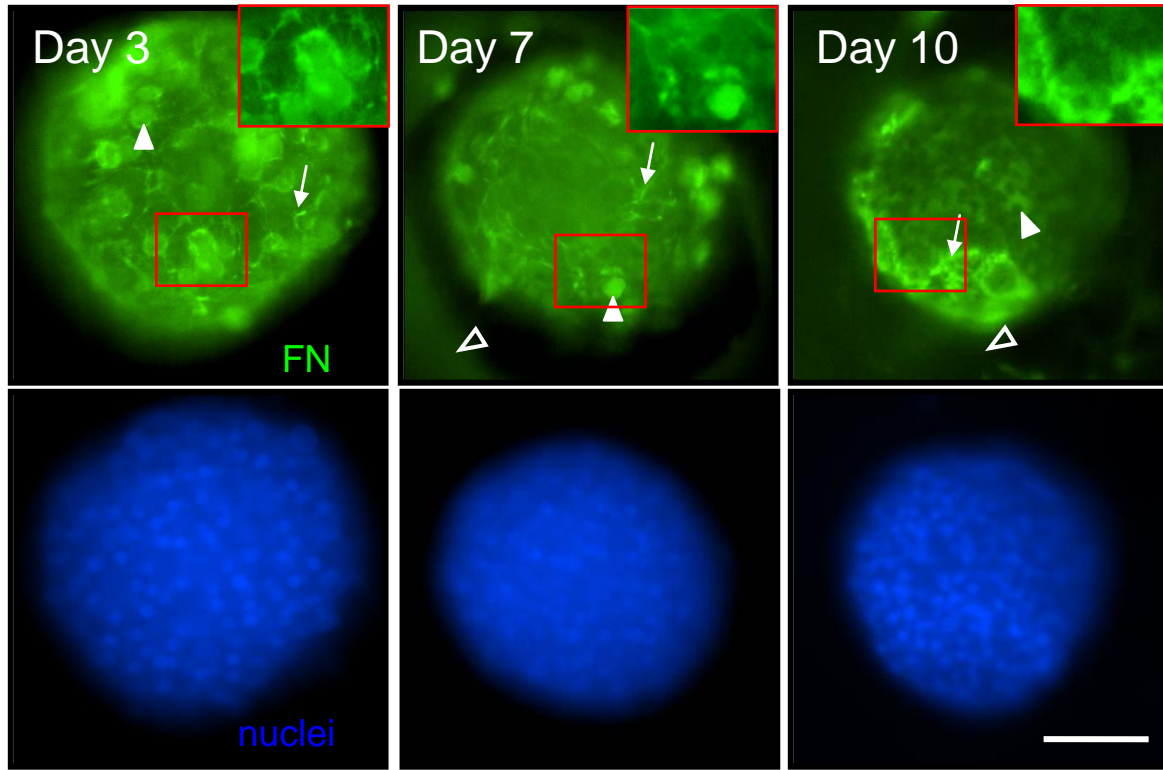


**Figure 2: Primary hepatocytes retain fibronectin matrix within micropatterned wells.**

Primary hepatocytes were plated as previously described. At 3, 7, and 10 days, cells were fixed and stained for fibronectin (green) and nuclei (blue). Confocal images were taken at 20X and digital zoom of red highlighted regions is illustrated in top right insets. Single confocal cross-sections taken within the centermost 25% of the structure are depicted. Note intracellular fibronectin (arrowheads), fibronectin fibrils (arrows) and staining for secreted, soluble fibronectin trapped in the walls of the microwell (open arrowheads). (For phase images see Figures 1 and 6 (day 3), Figure S4 (day 7) and Figure S5 (day10)). Scale bar = 100  $\mu\text{m}$ .

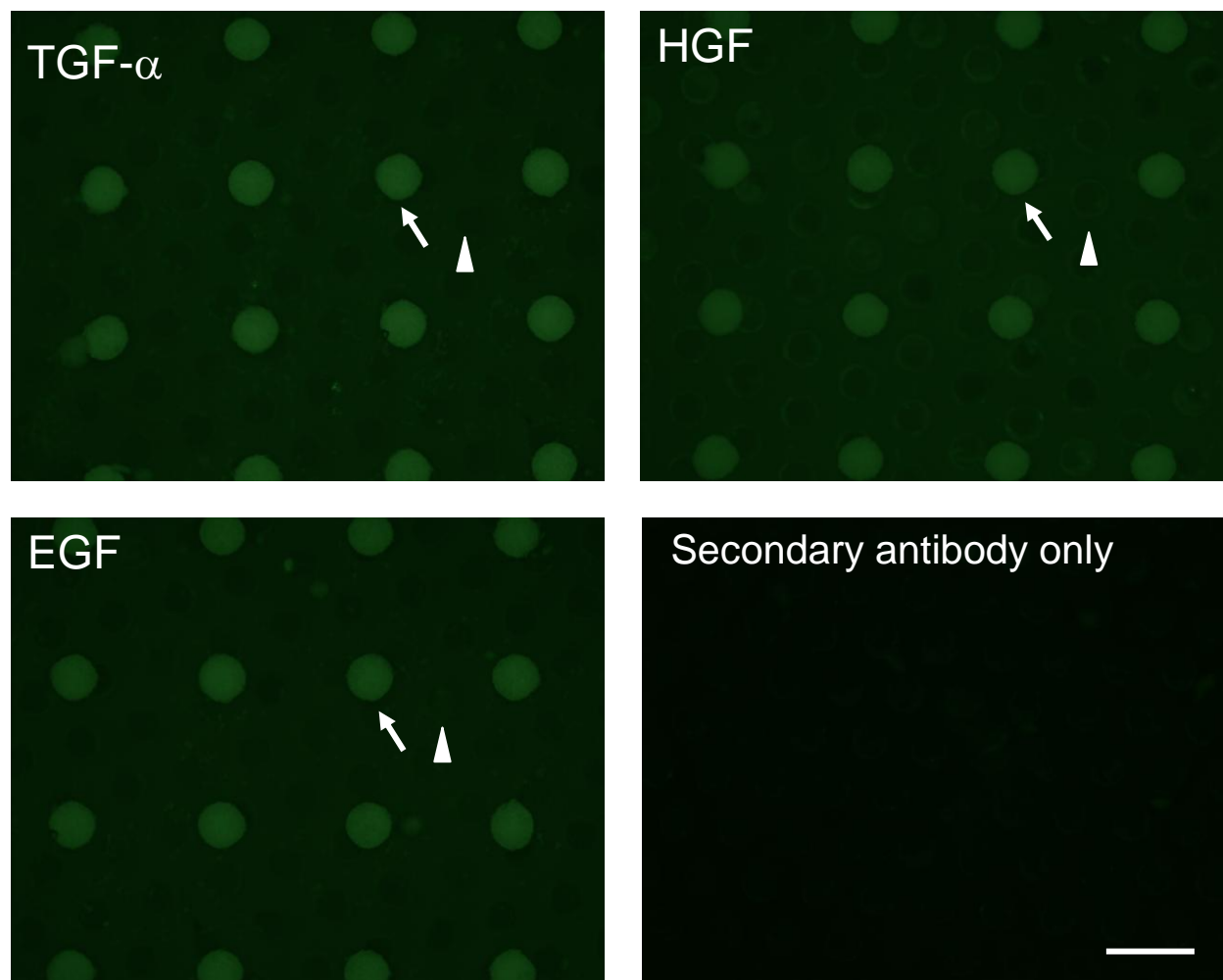


**Figure 3: Primary hepatocytes retain autocrine growth factors in micropatterned wells.**

Cells were cultured as previously described, in the absence of serum or exogenous growth factors (except for insulin). After three days, samples were fixed and stained with antibodies against EGF, HGF, and TGF- $\alpha$ . As a negative control, a sample was incubated with secondary antibody alone to confirm that signal was from primary antibody. Fluorescence indicates retention of TGF- $\alpha$ , EGF, and HGF. Microwells filled with cells are indicated by arrow, support scaffold channels are indicated arrowhead. Support scaffold channels are  $d=340\ \mu\text{m}$ , scale bar = 1mm (Magnification 35 X). For days 7 and 10, see Supplemental Figure S2.

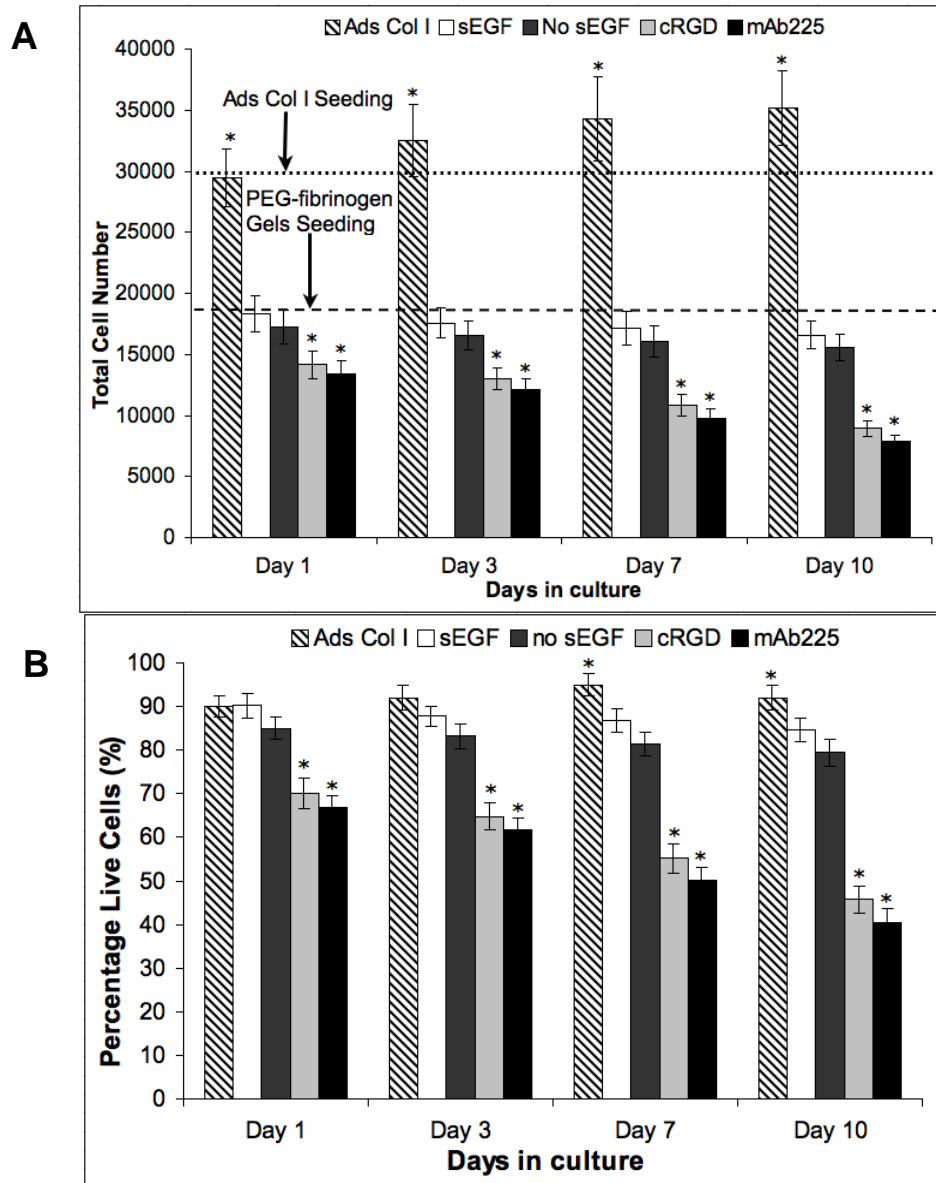


**Figure 4: Autocrine signaling is necessary and sufficient for the survival of primary hepatocytes *in vitro*.** **A)** Total cell numbers as a function of time in culture, **B)** Quantification of cell viability expressed as percentage of viable cells. Freshly isolated primary hepatocytes were plated onto molded gels at a density of 100,000 cells/cm<sup>2</sup> in hepatocyte growth medium with 10ng/ml EGF (white, sEGF), no EGF (dark grey, no EGF), no EGF with 10 $\mu$ M cyclic RGD peptide (light grey, cRGD), or no EGF with 10 $\mu$ M mAb225 (black, mAb225). Hepatocytes were cultured on adsorbed collagen I at a density of 100,000 cells/cm<sup>2</sup> in hepatocyte growth medium supplemented with 10ng/ml EGF (diagonal pattern, Ads Col I). At the indicated time-points, viable cells were identified by their ability to exclude Ethidium Bromide and total cell numbers were determined with DAPI staining. The horizontal lines depict total number of cells seeded on PEG-Fibrinogen gels and adsorbed collagen substrates. For PEG-Fibrinogen gels, total number of cells effectively seeded into 35 microwells per culture is based on measurements of the number of nuclei in 20 microwells in 4 samples 24 hr after plating. \* indicates statistical significance as compared to PEG gel soluble EGF condition on that specific day,  $p < 0.05$ ,  $n > 3$ .

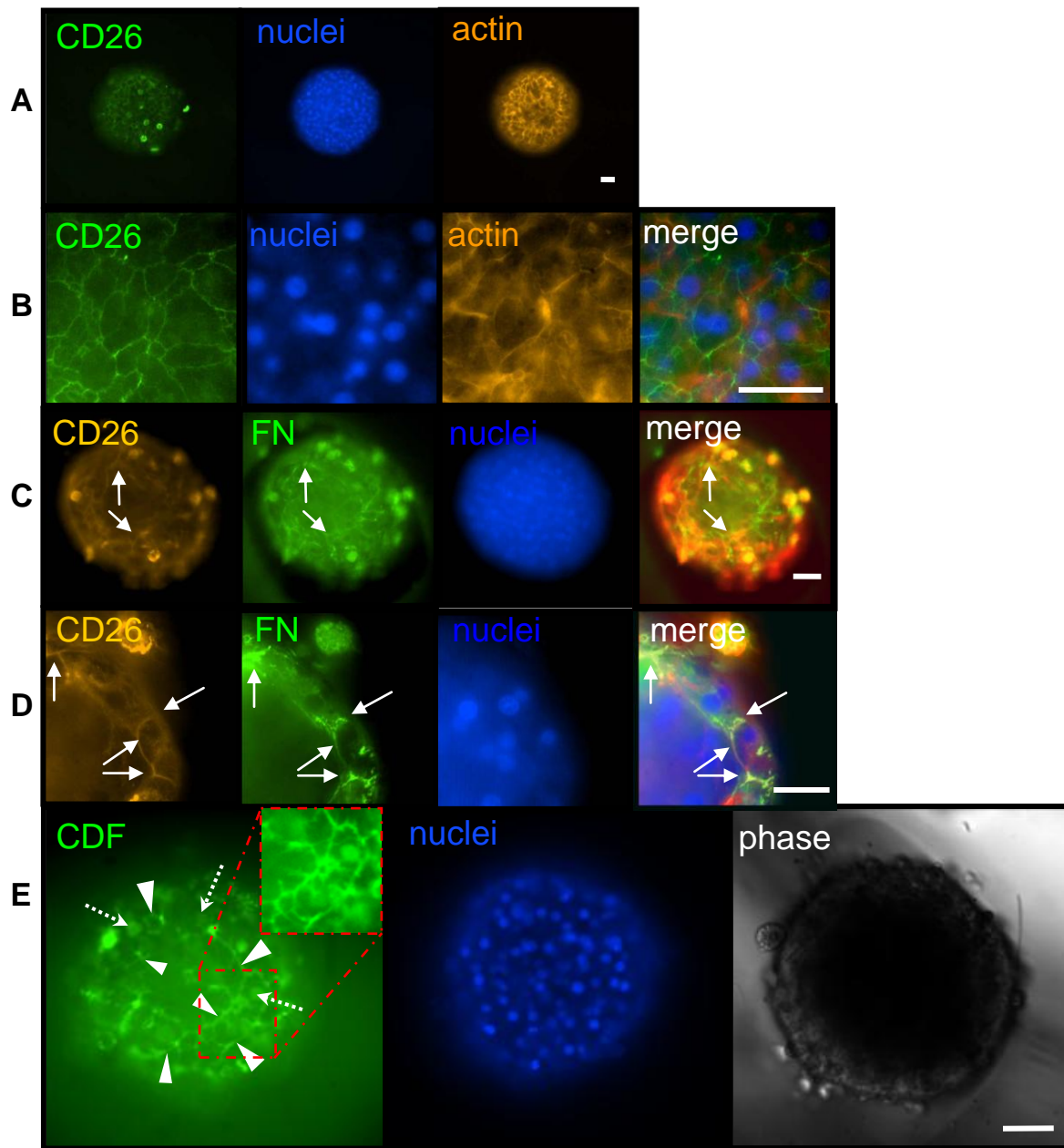


**Figure 5: Micropatterned PEG-Fibrinogen hydrogels support 3D polarization of primary hepatocytes and the formation of a functional bile canalicular network.** Cells were plated and cultured in hepatocyte growth medium without EGF as previously described, then fixed and stained for the indicated epitopes. Single confocal cross-sections taken within the centermost 25% of the structure are depicted. **A** and **B**, Cells cultured for 3 days and stained for CD26 (green), nuclei (blue), and the actin cytoskeleton (orange), samples imaged at 10X (**A**) and 63X (**B**). **C** and **D**, Cells cultured for 7 days and stained for CD26 (orange), fibronectin (green), and nuclei (blue), samples imaged at 20X (**C**) and 40X (**D**). **E**, Visualization of functional bile canaliculi by confocal microscopy on day 6 using 5 (and 6)-carboxy-2',7'-dichlorofluorescein (CDF) diacetate at 20X (with digital zoom of red highlighted region in top right inset). For reference, support scaffold channels are  $d=340\ \mu\text{m}$ . Scale bar =  $50\ \mu\text{m}$  in each image. Note regions of plasma membrane showing CD26 and fibronectin colocalization (arrows), and

---

concentrated CDF staining in the 3-D tissue structure which is similar to CD26 staining in **5A** and **5B** (arrowheads = bile canaliculi, dotted arrows = intracellular uptake of CDF).

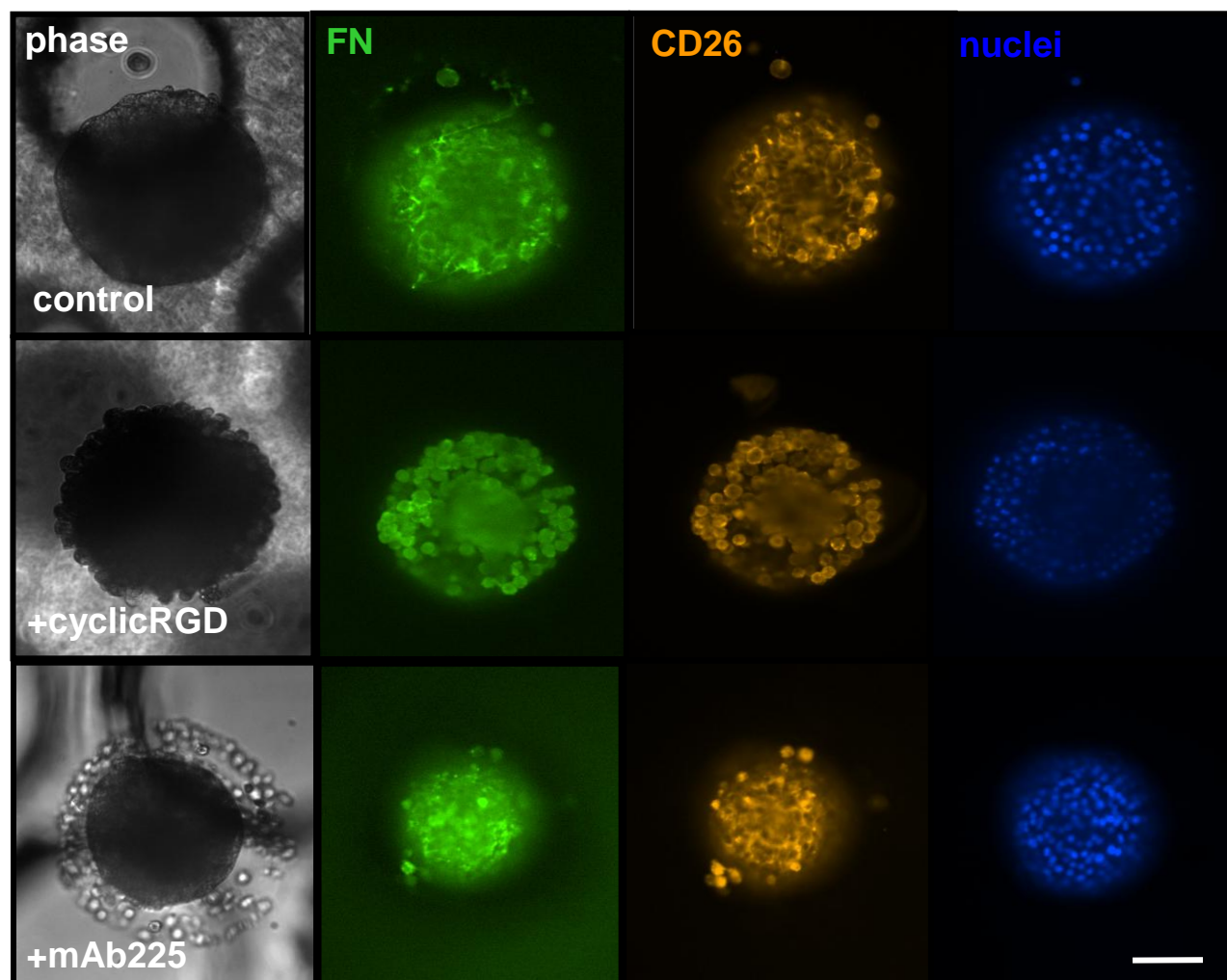


**Figure 6: Blocking  $\alpha 5\beta 1$  but not EGFR disrupts tissue-like structures.** Cells were plated as described above and cultured for 3 days in the absence or presence of 10  $\mu$ M cyclic RGD peptide or mAb225. After 3 days, cultures were fixed and stained for fibronectin (green), CD26 (orange), and nuclei (blue). Note the absence of fibronectin fibrils or discrete CD26 staining and the loose, dissociated cells in the microwells of cultures with cyclic RGD. Also note the smooth edges of the aggregates, loose cells in the bottom of the well, and staining for fibronectin and CD26 similar to control culture in the microwells of cultures with mAb225. For reference, support scaffold channels are  $d=340 \mu\text{m}$ . Scale bar = 100  $\mu\text{m}$ . For days 7 and 10, see Supplementary Figures S4 and S5.

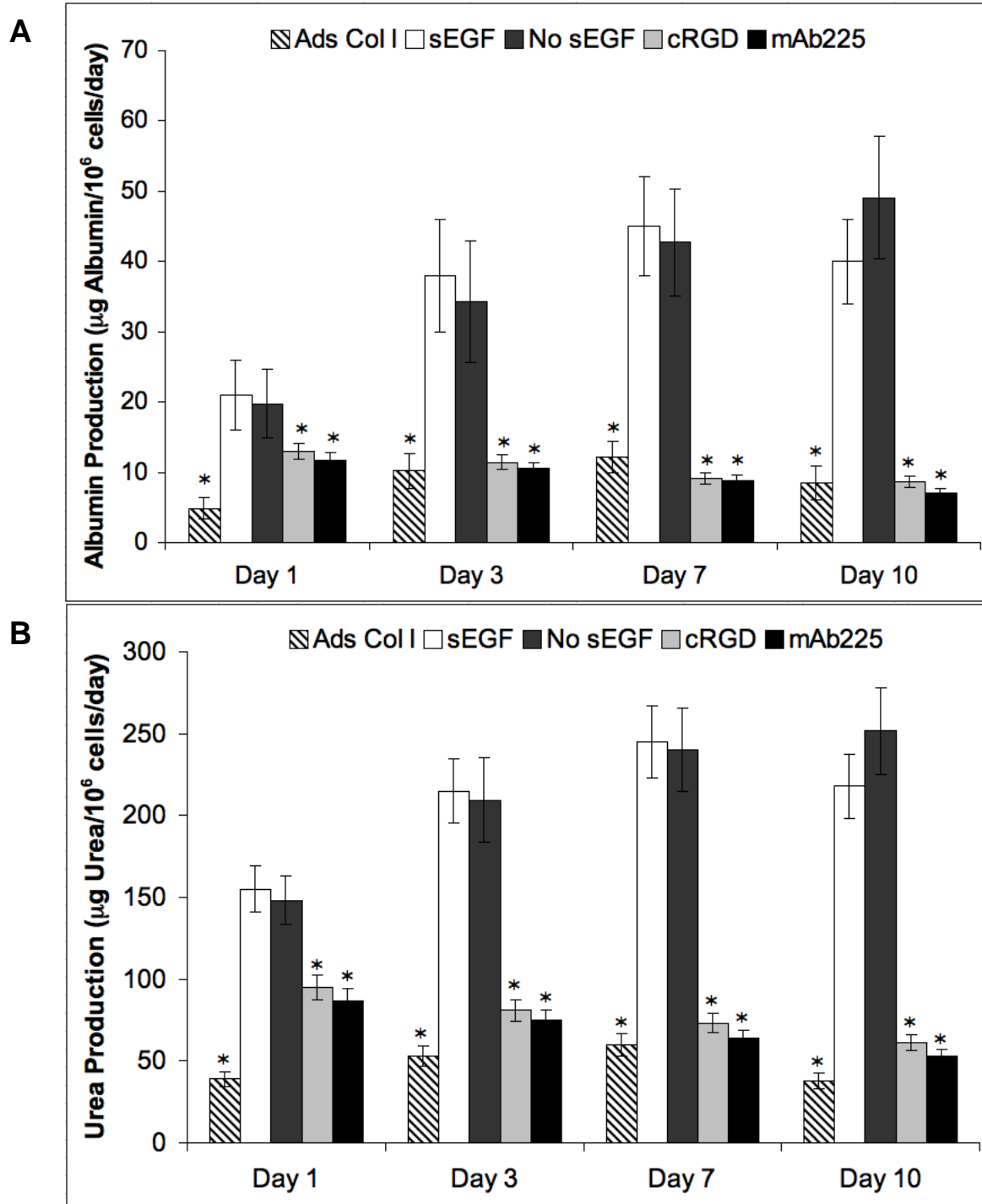


**Figure 7: PEG-Fibrinogen hydrogels promote maintenance of hepatocyte metabolic functions *in vitro*.** Primary hepatocytes were cultured on micromolded PEG-Fibrinogen gels or adsorbed collagen I as described in Materials and Methods. Conditioned medium was collected at the indicated time-points and metabolites of interest were quantified as described in Materials and Methods. Samples, standards, and controls were tested in duplicate. **A)** Albumin synthesis, **B)** Urea synthesis. \*indicates statistically significant difference from sEGF supplemented PEG-

---

Fibrinogen samples at a specific day,  $p < 0.05$ ,  $n > 3$ . For absolute (non-normalized) rates of secretion, see Supplementary Figure S6.

Tissue Engineering Part A  
Autocrine-controlled formation and function of tissue-like aggregates by primary hepatocytes in micropatterned hydrogel arrays (doi: 10.1089/ten.TEA.2010.0398)  
This article has been peer-reviewed and accepted for publication, but has yet to undergo copyediting and proof correction. The final published version may differ from this proof.